Hawkins et al., http://www.jcb.org/cgi/content/full/jcb.201004152/DC1

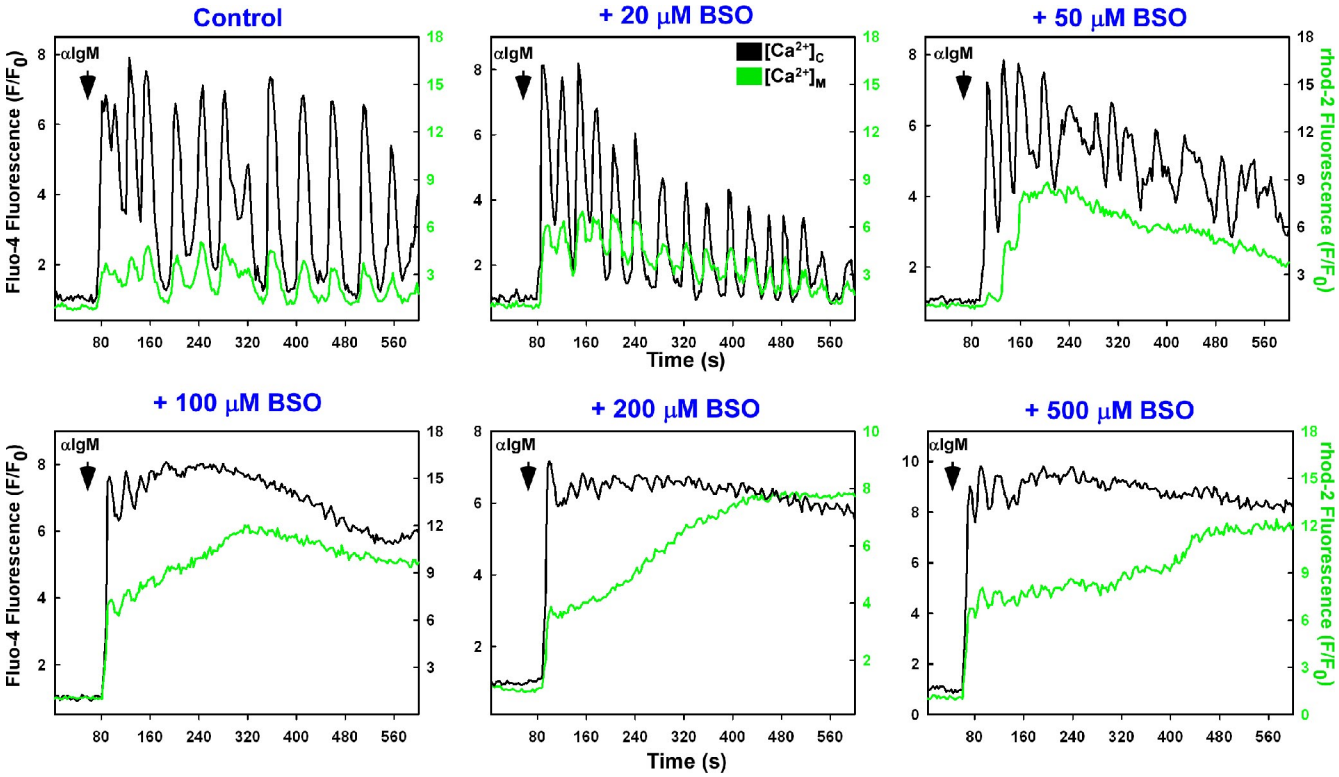

Figure S1. **Dose-dependent alterations in αIgM-induced calcium mobilization and mitochondrial calcium uptake in response to increasing concentrations of BSO.** DT40 cells were incubated with the indicated concentration of BSO for 24 h and loaded with Fluo-4 and rhod-2 to visualize cytosolic and mitochondrial calcium concentration, respectively. Images were collected every 3 s via confocal microscopy. Traces indicate fluorescence changes over time in response to 1.5 μg/ml αIgM. αIgM addition is noted by arrows.

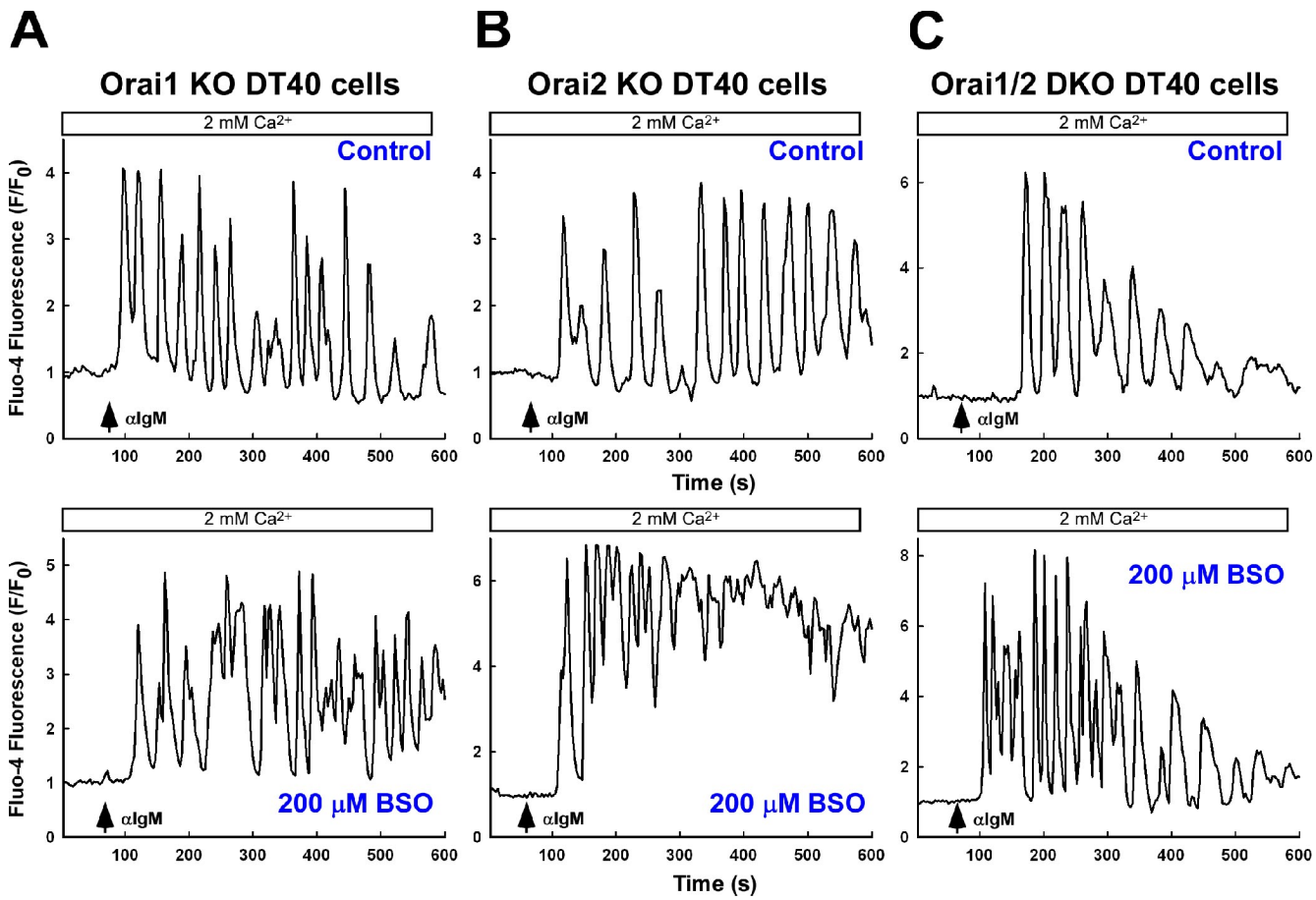

Figure S2. **Orai1 is requisite for the phenotypic alteration in calcium mobilization observed during oxidative stress.** DT40 cells were loaded with the calcium indicator dye Fluo-4, stimulated with 1.5 μg/ml αIgM, and fluorescence recorded every 3 s via confocal microscopy. Fluorescence values were normalized to baseline. (A) Orai1 KO DT40 cells exhibit an oscillatory calcium mobilization pattern in response to αIgM both in control and after 24-h treatment with 200 μM BSO. (B) After BSO challenge, Orai2 KO cells display a shift in the αIgM-induced calcium mobilization pattern from an oscillatory to a sustained phenotype. (C) Orai1/2 double-KO (DKO) cells are insensitive to BSO-induced oxidative stress. DT40 cells do not express Orai3. αIgM addition is noted by arrows.

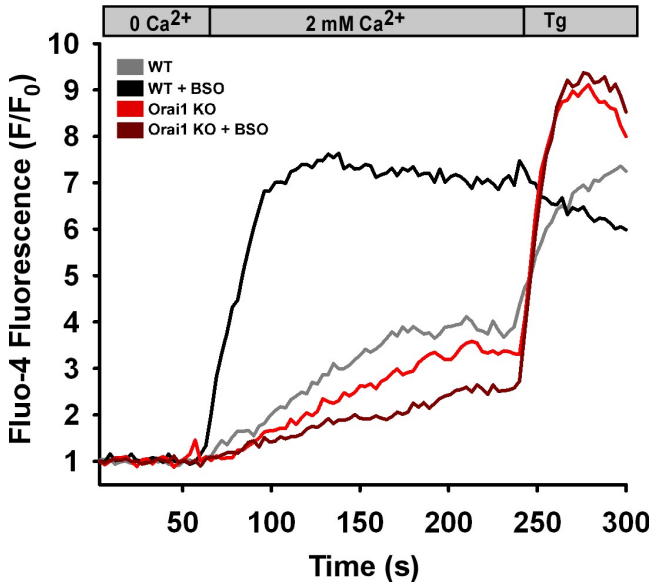

Figure S3. **Restoration of transient mitochondrial calcium uptake by elimination of capacitative calcium entry.** DT40 cells challenged with 200 μM BSO were loaded with Fluo-4 and rhod-2 and imaged via confocal microscopy. (A and B) αIgM activated calcium mobilization and mitochondrial calcium uptake in WT DT40 cells in the presence (A) and absence (B) of extracellular calcium. 2 mM calcium was added to activate capacitive calcium entry as indicated. (C) Calcium mobilization and mitochondrial calcium uptake in STIM1 KO DT40 cells in response to αIgM with and without extracellular calcium.

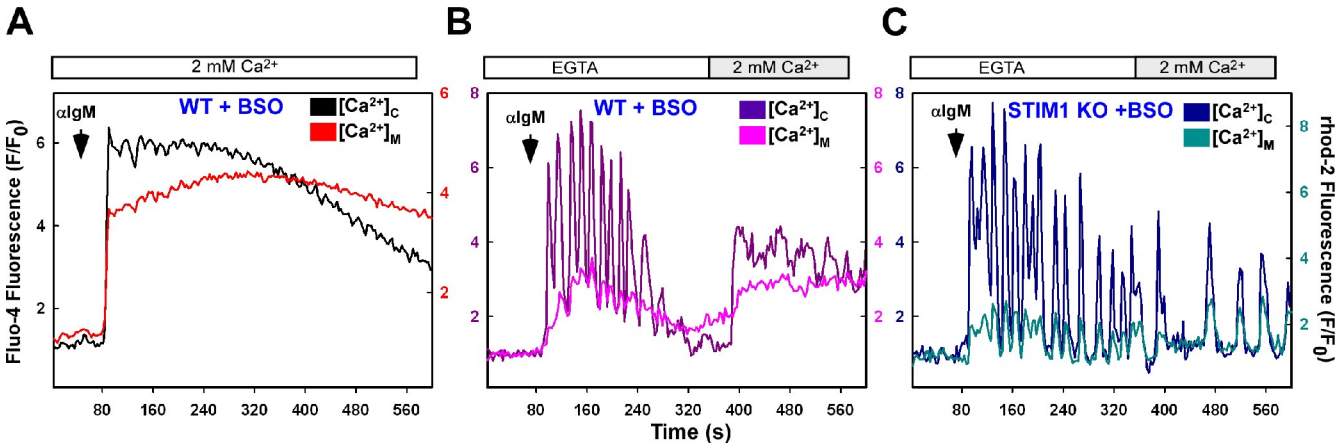

Figure S4. **Orai1 KO cells do not exhibit calcium entry in response to BSO.** WT and Orai1 KO DT40 cells were plated onto coverslips and loaded with Fluo-4 to assess calcium entry. WT, but not Orai1 KO DT40 cells, exhibited constitutive calcium entry when 2 mM calcium was added to the experimental buffer after BSO challenge (200 μM; 24 h). αIgM addition is noted by arrows.

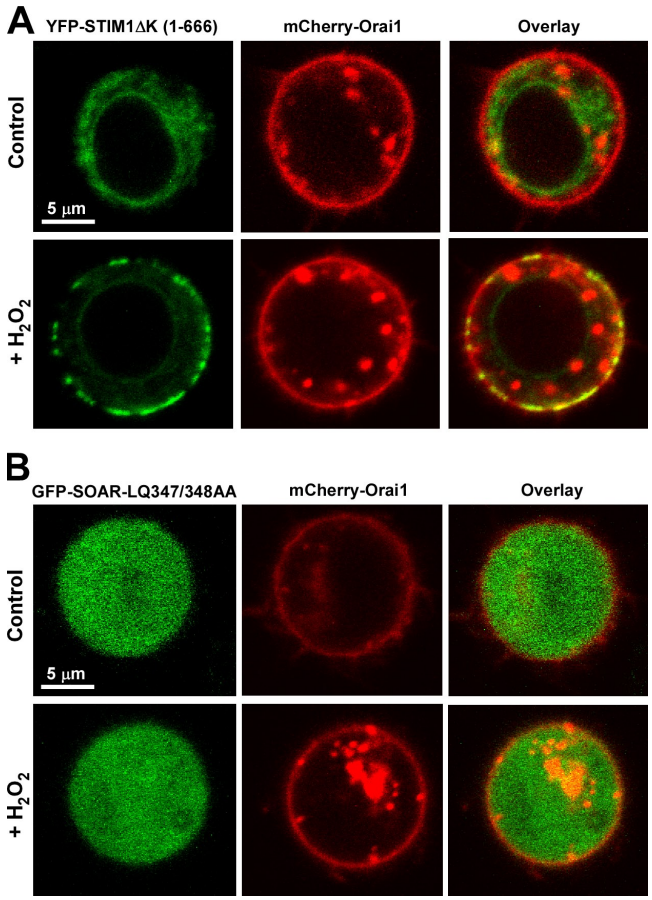

Figure S5. **Puncta formation under oxidant stress is dependent on the STIM1 N-terminal region.** (A) DT40 STIM1 KO cells were cotransfected with the YFP-tagged mutant STIM1 construct STIM1ΔK (1–666), which lacks K-rich lipid-binding region, and Orai1-mCherry. Images were collected in live cells under normal and oxidative conditions (+100 μM H_2O_2; 30 min) via confocal microscopy. STIM1 puncta were visible in the absence of Orai1 binding under oxidative stress conditions. (B) DT40 cells were cotransfected with the GFP-tagged mutant STIM1 construct SOAR-LQ347/348AA, which lacks the ER-luminal portion of the STIM1 protein and the Orai1-binding region, and Orai1-mCherry. Images were collected in live cells under normal and oxidative conditions (+100 μM H_2O_2; 30 min) via confocal microscopy. No STIM1 oligomerization occurred when the ER-luminal portion of STIM1 protein was not present under oxidative stress conditions.